Making Massless Dirac Fermions from a Patterned Two-Dimensional Electron Gas

Cheol-Hwan Park and Steven G. Louie*
Department of Physics, University of California at Berkeley, Berkeley, California 94720
Materials Sciences Division, Lawrence Berkeley National Laboratory, Berkeley, California 94720
(Dated: May 13, 2009)

Analysis of the electronic structure of an ordinary two-dimensional electron gas (2DEG) under an appropriate external periodic potential of hexagonal symmetry reveals that massless Dirac fermions are generated near the corners of the supercell Brillouin zone. The required potential parameters are found to be achievable under or close to laboratory conditions. Moreover, the group velocity is tunable by changing either the effective mass of the 2DEG or the lattice parameter of the external potential, and it is insensitive to the potential amplitude. The finding should provide a new class of systems other than graphene for investigating and exploiting massless Dirac fermions using 2DEGs in semiconductors.

Graphene[1,2,3,4], a honeycomb lattice of carbon atoms, is composed of two equivalent sublattices of atoms. The dynamics of the low-energy charge carriers in graphene may be described to a high degree of accuracy by a massless Dirac equation with a two-component pseudospin basis which denotes the amplitudes of the electronic states on these two sublattices. The quasiparticles have a linear energy dispersion near the corners $\mathbf{K}$ and $\mathbf{K}'$ (the Dirac points) of the hexagonal Brillouin zone[5,6,7,8]. Consequently, the density of states (DOS) varies linearly and vanishes at the Dirac point energy. The sublattice degree of freedom of the wavefunctions is given by a pseudospin vector that is either parallel or anti-parallel to the wavevector measured from the Dirac point, giving rise to a chirality being 1 or -1, respectively[5,6,7]. These two fundamental properties of graphene, linear energy dispersion and the chiral nature of the quasiparticles, result in interesting phenomenon such as half-integer quantum Hall effect[2,3], Klein paradox[9], and suppression of backscattering[6,7,10], as well as some novel predicted properties such as electron supercollimation in graphene superlattices[11,12,13].

As a possible realization of another two-dimensional (2D) massless Dirac particle system, theoretical studies on the physical properties of particles in optical honeycomb lattices[14] have been performed[15,16,17,18,19]. The behaviors of ultra-cold atoms in a honeycomb lattice potential were considered, in principle, to be equivalent to those of the low-energy charge carriers in graphene[15].

In this Letter, we propose a different practical scheme for generating massless Dirac fermions. We show through exact numerical calculations within an independent particle picture that applying an appropriate nanometer-scale periodic potential with hexagonal symmetry onto conventional two-dimensional electron gases (2DEGs) will generate massless Dirac fermions at the corners of the supercell Brillouin zone (SBZ). We find that the potential configurations needed should be within or close to current laboratory capabilities, and this approach could benefit from the highly developed experimental techniques of 2DEG physics[20] including recent advances in self-assembly nanostructures[21,22,23].

We moreover find that the band velocity and the energy window within which the dispersion is linear may be varied by changing the superlattice parameters or the effective mass of the host 2DEG, thus providing a different class of massless Dirac fermion systems for study and application. Interestingly, the amplitude of the periodic potential does not affect the band velocity about the Dirac points. But, if the external periodic potential is too weak, there is no energy window within which the DOS vanishes linearly. The linear energy dispersion and the chiral nature of states around the Dirac points of these 2DEG superlattices are found to be identical to those of graphene. Also, the associated up and down pseudospin states naturally correspond to states localizing, respectively, on two equivalent sublattice sites formed by the superlattice potential.

In order to investigate the properties of charge carriers in 2DEGs under an external periodic potential, we work within the one-electron framework with realistic material parameters. However, the point of this Letter is not the methodology itself, but the new idea and its feasibility. The study makes a connection between two of the largest and most active fields in condensed matter physics and nanoscience these days, graphene and 2DEGs, and provides experimentalists working on 2DEGs with a previously unexploited way of generating a new class of 2D massless Dirac fermions and of tuning their properties.

Let us consider a 2DEG with $E(\mathbf{p}) = p^2/2m^*$ where m^* is the electron effective mass. This is a good approximation to the energy dispersion of the lowest conduction band in diamond- or zinc-blende-type semiconductor quantum wells, which have effective masses ranging from $m^* = 0.02\ m_e \sim 0.17\ m_e$ where m_e is the free electron mass[24]. We shall consider explicitly two cases in the numerical calculations: $m^* = 0.02\ m_e$ and $m^* = 0.04\ m_e$.

Figure 1(a) shows the muffin-tin periodic potential considered in our numerical calculations, whose value is $U_0\,(>0)$ in a triangular array of disks of diameter d and zero outside. Figure 1(b) is the corresponding Brillouin zone. The muffin-tin form is chosen for ease of discussion; the conclusions presented here are generally valid for any hexagonal potential.

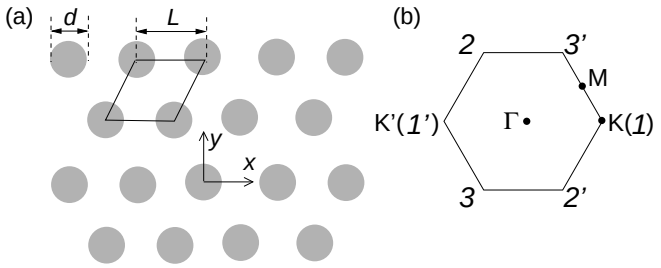

FIG. 1: (a) A muffin-tin type of hexagonal periodic potential with a spatial period L. The potential is $U_0\,(>0)$ inside the gray disks with diameter d and zero outside. (b) The Brillouin zone of hexagonal lattice in (a).

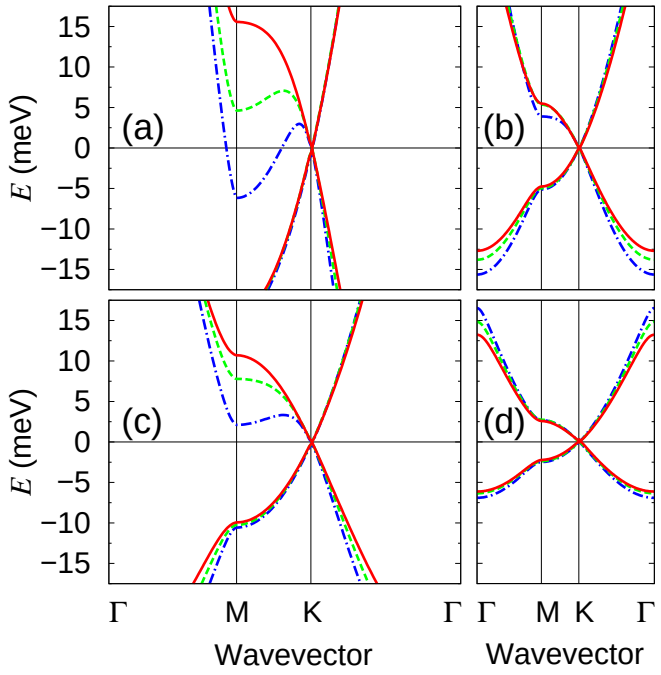

FIG. 2: (color online). Calculated energy bandstructure of the lowest two bands of a hexagonal 2DEG superlattice shown in Fig. 1(a). (a) $m^* = 0.02\,m_e$ and $L = 20$ nm, (b) $m^* = 0.02\,m_e$ and $L = 40$ nm, (c) $m^* = 0.04\,m_e$ and $L = 20$ nm, and (d) $m^* = 0.04\,m_e$ and $L = 40$ nm. The diameter of the disks d is set to $d = 0.663\,L$ (see text). Solid red, dashed green, and dash-dotted blue lines show results for U_0 equal to 200 meV, 100 meV, and 50 meV, respectively. The Dirac point energy (i. e. , the energy at the crossing of the two bands at $\mathbf{K}$) is set to zero.

We shall first discuss our numerical results and later consider the approximate analytic solutions. Figure 2 shows the calculated bandstructures of the lowest two bands for several hexagonal 2DEG superlattices with different effective mass m^*, lattice parameter L (with potential barrier diameter $d = 0.663\,L$[25]), and barrier height U_0. As the barrier height is decreased, the energy window within which the energy dispersion is linear is reduced (Fig. 2). (The potential barrier heights used in our calculations are typical of values employed in confining 2DEGs[20].) However, the group velocity at the Dirac point is insensitive to U_0 (Fig. 2). But, as m^* or L is increased, the group velocity decreases (Fig. 2).

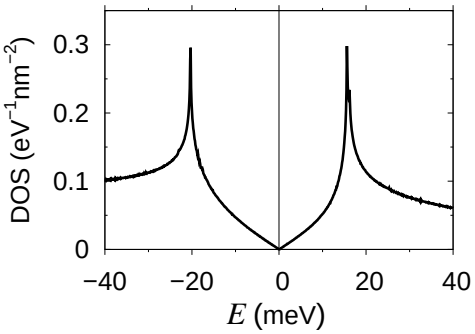

FIG. 3: The DOS of a triangular 2DEG superlattice with $m^* = 0.02\,m_e$, $U_0 = 200$ meV, $L = 20$ nm and $d = 13.3$ nm. (The zero of energy is set at the Dirac point.) The charge density needed to fill the conduction band up to the Dirac point energy is 5.7×10^{11} cm^{-2}.

Figure 3 shows the DOS of a hexagonal 2DEG superlattice with $m^* = 0.02\,m_e$, $U_0 = 200$ meV, $L = 20$ nm and $d = 13.3$ nm. The DOS has a linear behavior around the Dirac point energy within a ~ 30 meV energy window. The charge density required to dope the system to reach the Dirac point energy is 5.7×10^{11} cm^{-2}, which is in the range of typical value in 2DEG studies[20], and may be tuned by applying a gate voltage or by light illumination[26].

With the above results established from the numerical calculations, to gain further insight, we now present analytical expressions for the energy dispersion relation and wavefunctions around the SBZ corners obtained from degenerate perturbation theory. We concentrate on states with wavevector $\mathbf{k} + \mathbf{K}$ near the $\mathbf{K}$ point in the SBZ, i. e. , $|\mathbf{k}| \ll |\mathbf{K}|$. Let us set the energy of the empty lattice bandstructure at the $\mathbf{K}$ point to zero, define W as the Fourier component of the periodic potential connecting $1 \to 2$, $2 \to 3$ and $3 \to 1$ in Fig. 1(b)[25], and denote v_0 as the group velocity of the electron state at the $\mathbf{K}$ point of the 2DEG before applying the periodic potential. [For $E(\mathbf{p}) = p^2/2m^*$, $v_0 = \hbar K/m^*$. However, the derivation below is not confined to a quadratic energy dispersion for the original 2DEG.] Due to the inversion symmetry of the system considered here, W is real. The wavefunction $\psi_{\mathbf{k}}(\mathbf{r})$ may be approximately expressed as a linear combination of three planewave states

$$\psi_{\mathbf{k}}(\mathbf{r}) = \frac{1}{\sqrt{3A_c}}\left[c_1 \exp\left(i(\mathbf{K}_1 + \mathbf{k})\cdot\mathbf{r}\right) + c_2 \exp\left(i(\mathbf{K}_2 + \mathbf{k})\cdot\mathbf{r}\right) + c_3 \exp\left(i(\mathbf{K}_3 + \mathbf{k})\cdot\mathbf{r}\right)\right], \quad (1)$$

where A_c is the area of the 2DEG and $\mathbf{K}_1$, $\mathbf{K}_2$ and $\mathbf{K}_3$ represent wavevectors at the SBZ corners *1*, *2* and *3*, respectively, in Fig. 1(b). Equivalently, we could express the eigenstate as a three-component column vector $\mathbf{c} =$

$(c_1, c_2, c_3)^{\mathrm{T}}$. Within this basis, the Hamiltonian H, up to first order in k, is given by $H = H_0 + H_1$, where

$$H_0 = W \begin{pmatrix} 0 & 1 & 1 \\ 1 & 0 & 1 \\ 1 & 1 & 0 \end{pmatrix} \tag{2}$$

and

$$H_1 = \hbar v_0\, k \begin{pmatrix} \cos\theta_{\mathbf{k}} & 0 & 0 \\ 0 & \cos\left(\theta_{\mathbf{k}} - \frac{2\pi}{3}\right) & 0 \\ 0 & 0 & \cos\left(\theta_{\mathbf{k}} - \frac{4\pi}{3}\right) \end{pmatrix} . \tag{3}$$

Here $\theta_{\mathbf{k}}$ is the polar angle of the wavevector $\mathbf{k}$ from the $+x$ direction.

The eigenvalues of the unperturbed Hamiltonian H_0 are

$$E_0 = -W,\ -W,\ 2W\,, \tag{4}$$

which are also the energies of the states of the superlattice at $\mathbf{k} = 0$. We now focus on the doubly-degenerate eigenstates with eigenvalue $-W$. We shall find the $\mathbf{k}$-dependence of the eigenenergies and eigenvectors of H corresponding to these two states within degenerate perturbation theory by treating H_1 as a perturbation, which is approximate for $\hbar\, v_0\, k < W$. Also, for a wavefunction in the form of Eq. (1) to give a good description of the actual wavefunction, the energy to the next planewave state [which is $\hbar^2(2K)^2/2m^* - \hbar^2K^2/2m^*$] should be smaller than W. Therefore, the approximation is valid within the regime $\hbar\, v_0\, k < W < \frac{3\hbar^2K^2}{2m^*}$, or, equivalently,

$$\frac{4\pi\hbar^2}{3m^*L}k < W < \frac{8\pi^2\hbar^2}{3m^*L^2}\,, \tag{5}$$

where we have used $K = 4\pi/3L$.

The two eigenvectors of H_0 with eigenvalue $-W$ are

$$\mathbf{c}_1 = \frac{1}{\sqrt{2}} \begin{pmatrix} 0 \\ 1 \\ -1 \end{pmatrix} \quad \text{and} \quad \mathbf{c}_2 = \frac{1}{\sqrt{6}} \begin{pmatrix} 2 \\ -1 \\ -1 \end{pmatrix} . \tag{6}$$

The term H_1, when restricted to the sub-Hilbert-space spanned by the two vectors in Eq. (6), is represented by a 2×2 matrix $\tilde{H}_1$

$$\tilde{H}_1 = \hbar\frac{v_0}{2} \begin{pmatrix} -k_x & -k_y \\ -k_y & k_x \end{pmatrix} , \tag{7}$$

where $k_x = k\cos\theta_{\mathbf{k}}$ and $k_y = k\sin\theta_{\mathbf{k}}$. After a similarity transform $M = U^\dagger \tilde{H}_1 U$ with

$$U = \frac{1}{2} \begin{pmatrix} 1+i & -1-i \\ -1+i & -1+i \end{pmatrix} , \tag{8}$$

we obtain

$$M = \hbar\frac{v_0}{2}\left(k_x\sigma_x + k_y\sigma_y\right) . \tag{9}$$

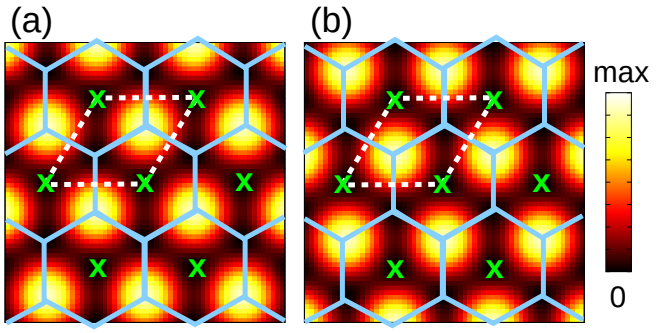

FIG. 4: (color online). Probability densities of the pseudospin states in a hexagonal 2DEG superlattice (a) $|\langle\mathbf{r}|\uparrow\rangle|^2$ and (b) $|\langle\mathbf{r}|\downarrow\rangle|^2$. Note that the amplitudes of the states are localized at two different but equivalent sublattices. The centers of the potential barrier disks [Fig. 1(a)] are shown as 'x' marks, and the honeycomb structure is drawn to illustrate the connection to the superlattice structure.

Here, σ_x and σ_y are the Pauli matrices. Equation (9) is just the effective Hamiltonian of graphene[5] with a group velocity

$$v_g = v_0/2 = \frac{\hbar K}{2m^*} = \frac{2\pi\hbar}{3m^*L}\,. \tag{10}$$

Therefore, the group velocity is reduced if the effective mass is increased or the lattice parameter of the superlattice is increased, but it is insensitive to the amplitude of the external periodic potential, which explains the results of the numerical calculations shown in Fig. 2. Also, the size of the linear energy dispersion window [Eq. (5)] is dictated by the value of W, which for the muffin-tin potential in Fig. 1(a) with $d = 0.663\,L$ is $W = 0.172\,U_0$[25] in agreement with the numerical calculations[27].

The eigenvalues and the eigenvectors of M are

$$E(s, \mathbf{k}) = s\,\hbar\frac{v_0}{2}\,k\,, \tag{11}$$

and

$$|s, \mathbf{k}\rangle = \frac{1}{\sqrt{2}} \begin{pmatrix} 1 \\ 0 \end{pmatrix} + \frac{1}{\sqrt{2}}\, s\, e^{i\theta_{\mathbf{k}}} \begin{pmatrix} 0 \\ 1 \end{pmatrix} , \tag{12}$$

respectively, where $s = \pm 1$ is a band index[5]. The vectors $\begin{pmatrix} 1 \\ 0 \end{pmatrix}$ and $\begin{pmatrix} 0 \\ 1 \end{pmatrix}$ are the up and the down pseudospin eigenstates of σ_z, respectively[28].

The up and the down pseudospin eigenstates may be expressed within the basis of the original Hamiltonian H using Eqs. (8) and (6) as

$$|\uparrow\rangle \;=\; \frac{1}{\sqrt{3}} e^{i\frac{3\pi}{4}} \left(1,\ e^{-i\frac{2\pi}{3}},\ e^{-i\frac{4\pi}{3}}\right)^{\mathrm{T}} \tag{13}$$

and

$$|\downarrow\rangle \;=\; \frac{1}{\sqrt{3}} e^{i\frac{3\pi}{4}} \left(1,\ e^{i\frac{2\pi}{3}},\ e^{i\frac{4\pi}{3}}\right)^{\mathrm{T}} , \tag{14}$$

respectively[29]. The real space pseudospin wavefunctions $\langle \mathbf{r}| \uparrow \rangle$ and $\langle \mathbf{r}| \downarrow \rangle$ are obtained by putting the coefficients in Eqs. (13) and (14) into Eq. (1). Figures 4(a) and 4(b) show $|\langle \mathbf{r}| \uparrow \rangle|^2$ and $|\langle \mathbf{r}| \downarrow \rangle|^2$, respectively. Note that the up and the down pseudospin states are seen as localized at one of the two equivalent sublattices formed by the external periodic potential, in perfect analogy with the behavior in graphene.

Let us now consider the Landau levels for the above hexagonal 2DEG superlattice in a magnetic field $\mathbf{B} = B\,\hat{z}$ when the Fermi level is at the Dirac point energy. In exact analogy with graphene, the low-energy Landau levels shifted by the energy W (i. e. , having the energy zero at the Dirac point energy) are $E_n = \hbar\omega_c\,\mathrm{sgn}(n)\sqrt{|n|}$, where $\omega_c = v_0\sqrt{|e|B/2\hbar c}$ is the cyclotron frequency[8,30]. Here, for an appropriately constructed superlattice potential, the half-integer quantum Hall effect[2,3] should be observable.

In conclusion, we have shown that chiral massless Dirac fermions are generated if an appropriate nanometer-scale periodic potential with hexagonal symmetry is applied to a conventional 2DEG in semiconductors. These quasiparticles have a linear energy dispersion, with a group velocity half the value of the states before applying the periodic potential, and a wavefunction whose chiral structure exactly the same as that of graphene. The up and the down pseudospin states are shown to be localized at two different but equivalent sublattices formed by the superlattice potential. The quasiparticle group velocity moreover is tunable by changing the effective mass of the original 2DEG or the lattice parameter of the superlattice potential. Our findings thus provide a new class of systems for experimental investigations and practical applications of 2D massless Dirac quasiparticles.

We thank Kathryn Todd, Ileana Rau, Sami Amasha, Philip Kim, Yunchul Chung, Jiwoong Park, and Jannik Meyer for fruitful discussions. This work was supported by NSF Grant No. DMR07-05941 and by the Director, Office of Science, Office of Basic Energy Sciences, Division of Materials Sciences and Engineering Division, U.S. Department of Energy under Contract No. DE-AC02-05CH11231. Computational resources have been provided by NPACI and NERSC.

Note added in proof. – After we finished writing up this manuscript, we became aware of Ref.[31] in which a similar methodology to the one developed independently here was developed. The objects of investigation (which are cold fermionic atoms confined in honeycomb optical lattices) and the main ideas and conclusions in Ref.[31], however, are qualitatively different from those in this Letter.

* Electronic address: sglouie@berkeley.edu

1. K. S. Novoselov, D. Jiang, F. Schedin, T. Booth, V. V. Khotkevich, S. V. Morozov, and A. K. Geim, Proc. Natl. Acad. Sci. USA. **102**, 10451 (2005).
2. K. S. Novoselov, A. K. Geim, S. V. Morozov, D. Jiang, M. I. Katsnelson, I. V. Grigorieva, S. V. Dubonos, and F. A. A., Nature **438**, 197 (2005).
3. Y. Zhang, J. W. Tan, H. L. Stormer, and P. Kim, Nature **438**, 201 (2005).
4. C. Berger, Z. Song, X. Li, X. Wu, N. Brown, P. N. First, and W. A. de Heer, Science **312**, 1191 (2006).
5. P. R. Wallace, Phys. Rev. **71**, 622 (1947).
6. T. Ando and T. Nakanishi, J. Phys. Soc. Jpn. **67**, 1704 (1998).
7. T. Ando, T. Nakanishi, and R. Saito, J. Phys. Soc. Jpn. **67**, 2857 (1998).
8. J. W. McClure, Phys. Rev. **104**, 666 (1956).
9. M. I. Katsnelson, K. S. Novoselov, and A. K. Geim, Nat. Phys. **2**, 620 (2006).
10. P. L. McEuen, M. Bockrath, D. H. Cobden, Y.-G. Yoon, and S. G. Louie, Phys. Rev. Lett. **83**, 5098 (1999).
11. C.-H. Park, L. Yang, Y. W. Son, M. L. Cohen, and S. G. Louie, Nature Phys. **4**, 213 (2008).
12. C.-H. Park, Y.-W. Son, L. Yang, M. L. Cohen, and S. G. Louie, Nano Lett. **8**, 2920 (2008).
13. C.-H. Park, L. Yang, Y.-W. Son, M. L. Cohen, and S. G. Louie, Phys. Rev. Lett. **101**, 126804 (2008).
14. G. Grynberg, B. Lounis, P. Verkerk, J.-Y. Courtois, and C. Salomon, Phys. Rev. Lett. **70**, 2249 (1993).
15. S.-L. Zhu, B. Wang, and L.-M. Duan, Phys. Rev. Lett. **98**, 260402 (2007).
16. C. Wu, D. Bergman, L. Balents, and S. D. Sarma, Phys. Rev. Lett. **99**, 070401 (2007).
17. C. Wu and S. D. Sarma, Phys. Rev. B **77**, 235107 (2008).
18. L. H. Haddad and L. D. Carr, arXiv:0803.3039v1.
19. L. B. Shao, S.-L. Zhu, L. Sheng, D. Y. Xing, and Z. D. Wang, Phys. Rev. Lett. **101**, 246810 (2008).
20. J. T. Devreese and F. M. Peeters, eds., *The Physics of the Two-Dimensional Electron Gas* (Plenum, New York, 1987).
21. E. Ribeiro, E. Müller, T. Heinzel, H. Auderset, K. Ensslin, G. Medeiros-Ribeiro, and P. M. Petroff, Phys. Rev. B **58**, 1506 (1998).
22. E. Ribeiro, R. D. Jäggi, T. Heinzel, K. Ensslin, G. Medeiros-Ribeiro, and P. M. Petroff, Phys. Rev. Lett. **82**, 996 (1999).
23. E. Ribeiro, R. Jäggi, T. Heinzel, K. Ensslin, T. G. Medeiros-Ribeiro, and P. M. Petroff, Microelectron. Eng. **61**, 674 (1999).
24. P. Y. Yu and M. Cardona, *Fundamentals of Semiconductors: Physics and Materials Properties* (Springer, New York, 2001).
25. The Fourier component W, defined to be the value of the external periodic potential [Fig. 1(a)] in Fourier space at the smallest reciprocal lattice vector, is given by $W = \frac{d}{2L} J_1\left(\frac{2\pi d}{\sqrt{3}L}\right) U_0$ where $J_1(x)$ is the first-order Bessel function. For a given U_0, the maximum value of W is $W = 0.172\,U_0$ at $d = 0.663\,L$. In our numerical calculations, we take advantage of this. For comparison, if $d = 0.5\,L$, $W = 0.145\,U_0$.

[26] C. Albrecht, J. H. Smet, D. Weiss, K. von Klitzing, R. Hennig, M. Langenbuch, M. Suhrke, U. Rössler, V. Umansky, and H. Schweizer, Phys. Rev. Lett. **83**, 2234 (1999).

[27] In fabricated 2DEG superlattices, small fluctuations will inevitably occur in the amplitude and periodicity of the potential. These have been studied theoretically (Refs.[32,33,34]) for systems with honeycomb symmetry (like graphene) and found to be of little effect on the DOS and transport properties at low concentrations. In particular, a recent *ab initio* study (Ref.[34]) of graphene shows insignificant changes in the linear behavior in the DOS around the Dirac point energy up to 5 % in concentration of boron and nitrogen impurities. We expect the same robustness should occur for the 2DEG superlattices.

[28] Similar procedures can be applied to find the energy and the wavefunction of massless Dirac fermions with wavevectors near $\mathbf{K}'$ [Fig. 1(b)].

[29] Putting Eqs. (13) and (14) into Eq. (12), we obtain, within a phase factor, the eigenvector in the original planewave coefficient basis [Eq. (1)]

$$\mathbf{c}(s,\mathbf{k}) = \begin{cases} \sqrt{\frac{2}{3}} \begin{pmatrix} \cos\left(\frac{\theta_{\mathbf{k}}}{2}\right) \\ \cos\left(\frac{\theta_{\mathbf{k}}}{2}+\frac{2\pi}{3}\right) \\ \cos\left(\frac{\theta_{\mathbf{k}}}{2}+\frac{4\pi}{3}\right) \end{pmatrix} & (s=1) \\ \\ \sqrt{\frac{2}{3}} \begin{pmatrix} \sin\left(\frac{\theta_{\mathbf{k}}}{2}\right) \\ \sin\left(\frac{\theta_{\mathbf{k}}}{2}+\frac{2\pi}{3}\right) \\ \sin\left(\frac{\theta_{\mathbf{k}}}{2}+\frac{4\pi}{3}\right) \end{pmatrix} & (s=-1) \end{cases}$$

.

[30] The expression for the (relativistic) Landau levels is valid when the spacing between Landau levels are much smaller than the size of the energy window within which the dispersion is linear, regardless of the existence of higher energy states, just as in graphene. For example, in a triangular 2DEG superlattice with $m^* = 0.02\, m_e$, $U_0 = 200$ meV, $L = 20$ nm and $d = 13.3$ nm, this condition is equivalent to $B < 2$ T.

[31] B. Wunsch, F. Guinea, and F. Sols, New J. Phys. **10**, 103027 (2008).

[32] S. Wu, L. Jing, Q. Li, Q. W. Shi, J. Chen, H. Su, X. Wang, and J. Yang, Phys. Rev. B **77**, 195411 (2008).

[33] B. Dóra, K. Ziegler, and P. Thalmeier, Phys. Rev. B **77**, 115422 (2008).

[34] A. Lherbier, X. Blase, Y.-M. Niquet, F. Triozon, and S. Roche, Phys. Rev. Lett. **101**, 036808 (2008).